Res. Rep. Fac. Eng. Mie Univ., Vol. 23, pp. 1 −12 (1998)

Original Paper

Effect of stress-relief annealing for preventing low-ductility creep-fracture of HAZ of Cr-Mo steel

Hiroshi KAWAKAMI, Koreaki TAMAKI, Jippei SUZUKI,
Nobuhiro AKAO and Shiro MORISAWA
(Department of Mechanical Engineering)

(Received September 16, 1998)

Abstract

Low-ductility creep-fracture (LDCF) occured occasionally in heat affected zone (HAZ) of Cr-Mo steels under long-time service. Effect of SR treatment for LDCF of 2 1/4Cr-1Mo and 1 1/4Cr-1/2Mo steel was investigated from the view point of improving ductility of specimen. LDCF was reproduced in laboratory by using synthetic HAZ specimen and creep-rupture test. Two types of intergranular fracture (Type I and Type II) were observed in fracture surfaces of specimens. SR treatment was carried out at 975K and 925K for 2 1/4Cr-1Mo and for 1 1/4Cr-1/2Mo steels, respectively. The time for SR treatment ranges from 2 to 200hr. Ductility of HAZ specimen was improved very much by SR treatment producing the ductile fracture of type III when the treating time was long enough. When the treating time was short, the ductility in short time range was large but it decreased in long time range producing the fracture of type II. The optimum condition of SR treatment is 20hr at 975K and 200hr at 925K for 2 1/4Cr-1Mo steel and for 1 1/4Cr-1/2Mo steel, respectively.

Key words: Cr-Mo steels, low-ductility creep fracture, heat affected zone, synthetic HAZ specimen, SR treatment, segregation of impurity, intergranular fracture, secondary hardening.

1. Introduction

Cr-Mo steels have good weldability and mechanical properties in the medium temperature range and used for constructing boilers and pressure vessels. Low-ductility creep-fracture (LDCF), however, occurred occasionally in heat affected zone (HAZ) of these welded constructions when they are used at the service temperatures around 800K [1-3]. Some welded constructions are used without stress-relief annealing (SR) treatment, and others are used after SR treatment [4]. This treatment may effectively improve the ductility in creep-fracture, as well as reduces the residual stress. The authors intended in this research to confirm the effect of SR treatment for preventing LDCF and determined the optimum SR condition for 2 1/4Cr-1Mo and 1 1/4Cr-1/2Mo steels.

LDCF in 2 1/4Cr-1Mo and 1 1/4Cr-1/2Mo steels was reproduced by creep-rupture test on the synthetic HAZ specimen [5]. The creep-ductility of SR-treated specimen was compared with that of HAZ specimen. Changes in Ductility and fracture modes of each specimen were measured with the lapse of time to fracture.

2. Experimental system

2.1 Simulated HAZ specimen

1 1/4Cr-1/2Mo and 2 1/4Cr-1Mo steels shown in Table 1 were used for experiment. A simulated HAZ specimen, instead of real HAZ, was used for creep-rupture test, because a real HAZ was narrow in area and slant to plate surface, and it was difficult to take out the test specimen from welded zone. The welded-thermal cycle, which was given to HAZ by the following arc welding constructions, was reproduced in a steel bar [5]. This thermal cycle produced a microstructure same as that of real HAZ in the as-welded state.

Table 1 Chemical compositions of steel plates used ,wt%.

Steel type	C	Si	Mn	P	S	Cr	Mo	As	N	Al_{sol}
2 1/4Cr-1Mo(A)	0.15	0.12	0.52	0.004	0.001	2.40	1.05	0.002	0.0059	0.015
1 1/4Cr-1/2Mo	0.15	0.74	0.60	0.005	0.003	1.40	0.52	0.002	0.0033	0.015

arc voltage 24V, welding current 180A, welding speed 15cm/min, heat input 17.3kJ/cm, a bead welding without preheating.

The microstructures of each steel are 25% martensite and 75% bainite for 2 1/4Cr-Mo steel and 20% martensite and 80% bainite for 1 1/4Cr-1/2Mo steel. The average diameter of prior-austenite grains of each specimen was 130μm.

2.2 Thermal cycle of SR treatment

The thermal histories given to two groups of simulated HAZ specimens are shown in Fig.1. One group was subjected directly to creep-rupture test. The other was subjected to the test after SR treatment.

The conditions of SR treatment were 975K for 2 to 200 hours for 2 1/4Cr-1Mo and 925K for 2 to 200 hours for 1 1/4Cr-1/2Mo steel. The specimens were cooled from SR treatment by water-quenching to avoid the embrittlement induced by the SR treatment [6]. The cooling rate is 4K/s.

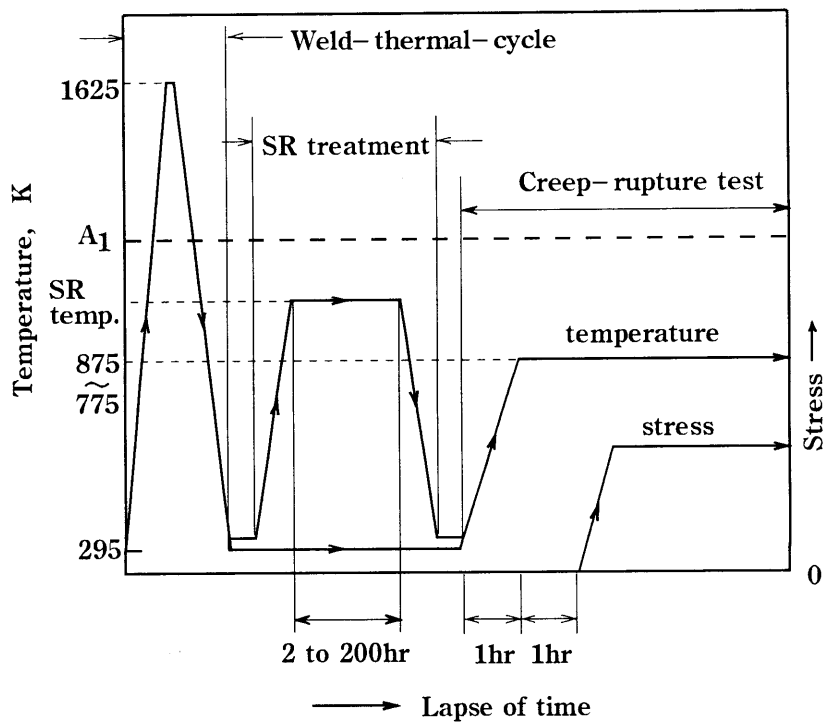

Fig.1 Two types of thrmal and loading histories in experiment.

2.3 Creep-rupture test

A notched specimen for creep-rupture test is shown in Fig.2. The uniform microstructure is produced in center portion of 20mm in length. The specimen was heated to test temperature of 775K or 825K in 1hr and kept for 1hr at this temperature before loading. The maximum fractuation from each given test temperature was 5K. The stresses of creep-rupture test were 200 to 800MPa.

The creep-rupture test was made also on the base metal specimen in as-received state.

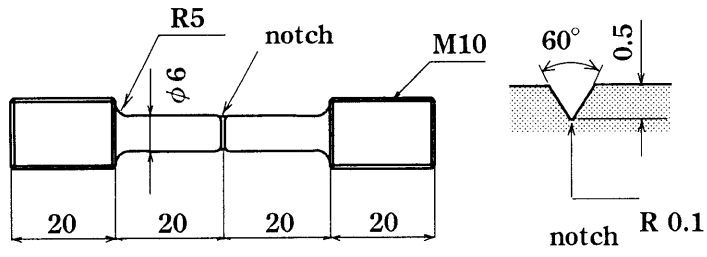

Fig.2 specimen for creep-rupture test.

3. Ductility and fracture mode of HAZ specimens

3.1 Ductility

The diagrams of stress and time to fracture of 1 1/4Cr-1/2Mo and 2 1/4Cr-1Mo steels are shown in Fig.3. The time to fracture at a given stress is longer for HAZ specimen than that of base metal specimen in a higher stress level. This relationship, however, is reversed in a lower stress level. Such the tendency shown above agrees the results of previous researches [1-3].

The reduction in area was measured to evaluate the ductility of fractured specimens. The reduction in area of each specimen is shown in Fig.4. The reduction in area of base metal speci-

men is large in short time range. It reduces, however, in the long time range. On the other hand, HAZ specimen exhibits a very small reduction in area, that is, the low-ductility creep-fracture.

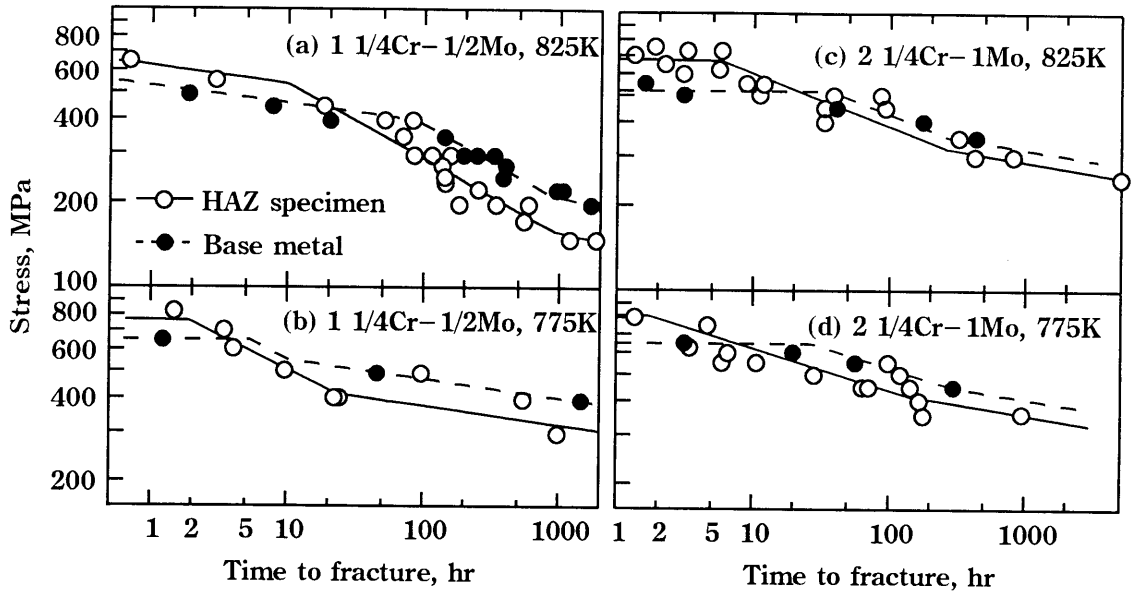

Fig.3 Results of creep-rupture test; HAZ specimens of 1 1/4Cr-1/2Mo and 2 1/4Cr-1Mo steels.

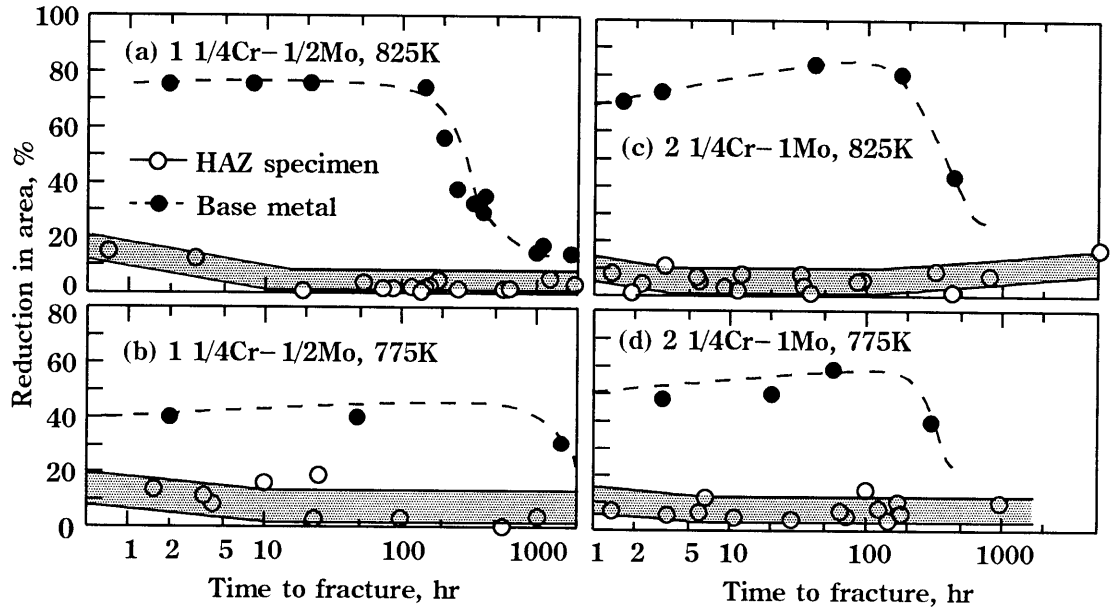

Fig.4 Change in reduction in area with increasing time to fractue; HAZ specimens of 1 1/4Cr-1/2Mo and 2 1/4Cr-1Mo steels.

3.2 Classification of fracture modes

Fracture surfaces of all specimen were observed by a SEM with magnifications of 100 to 500. Fracture modes were classified into three types by their appearance as shown in Fig.5. Typical features of each type of fracture are as follows.

Type I (Fig.5(a)): This type exhibits a typical intergranular fracture which occurs along grain boundaries of prior-austenite. The surfaces of each crystal grain are flat and smooth, and edges of each grain are very sharp.

Type II (Fig.5(b),(c)): This type of fracture occurs along grain boundaries of prior-

austenite as the case of type I, but it differs from that in the following special features: (1)each crystal grain is deformed in some extent, (2)a wavy pattern is observed on some surfaces of a grain, (3)some cracks run into the crystal grains. This fracture mode was observed at both of HAZ (Fig.5(b)) and SR-treated specimen (Fig.5(c)).

Type III (Fig.5(d)): This type belongs to the ductile fracture of transgranular mode. It is observed in all of fracture surface of base metal and some SR treated specimen with high ductility, and at center portion of fracture surface of HAZ and some SR treated specimen with low ductility.

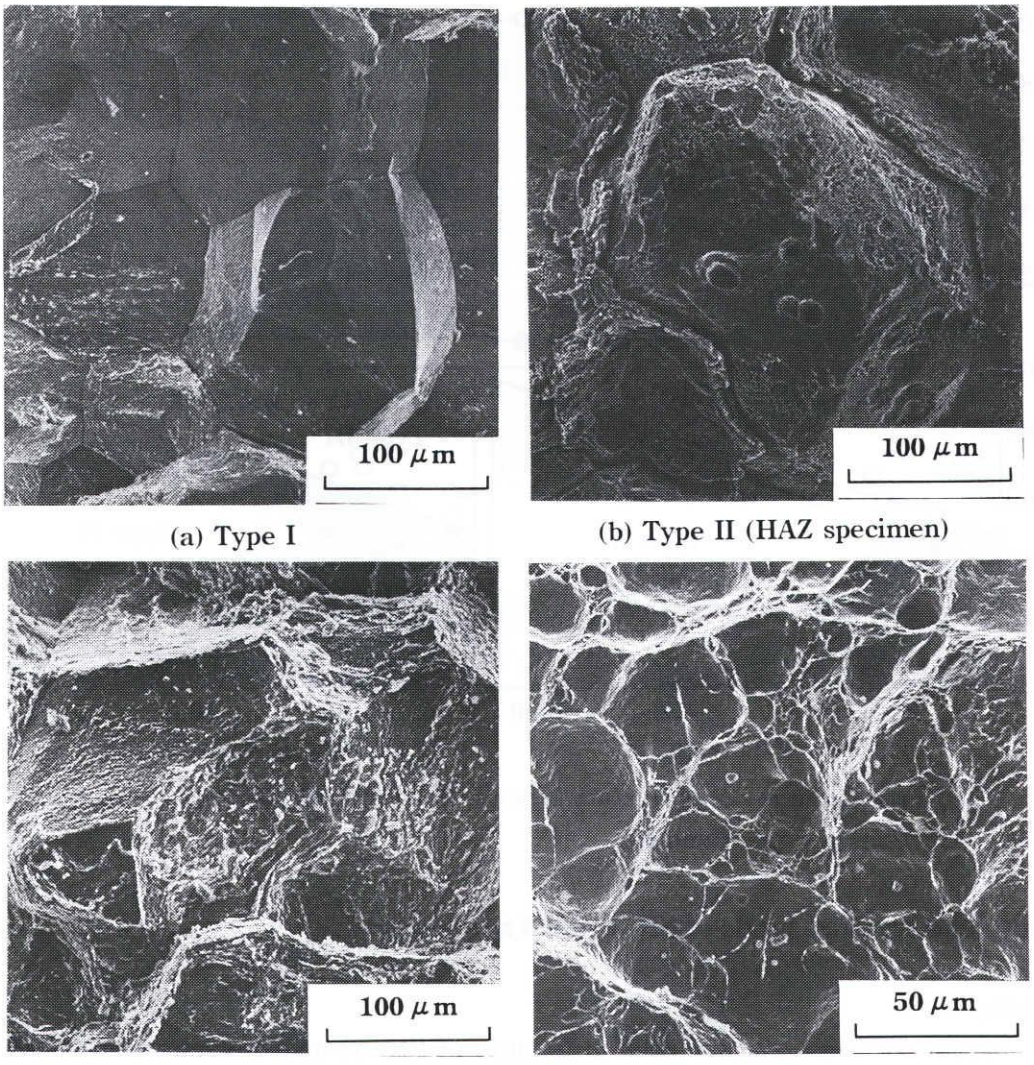

(a) Type I (b) Type II (HAZ specimen)

(c) Type II (SR-treated specimen) (d) Type III

Fig.5 Three types of fracture modes of HAZ and SR-treated specimens; 1 1/4Cr-1/2Mo steel, tested at 825K.

3.3 Change in fracture mode with the lapse of time to fracture

The area of three types of fracture modes were measured for all HAZ specimens of 1 1/4Cr-1/2Mo and 2 1/4Cr-1Mo steels. The Diagrams of the fraction of fracture type against the time to fracture are shown in Fig.6. The solid circle indicates the fraction of area of type I; The distance from the open circle to the solid one indicates the fraction of area of Type II.

In case of 1 1/4Cr-1/2Mo steel tested at 825 and 775K (Fig.6 (a) and (b)), types I and III were observed in short time range. The fraction of area of type I increases until certain time

period and then decreases to zero with the lapse of time. Type III is observed on the center portion of fracture surface for all specimens. Fraction of area of type III is large in short time range, but it decreases with lapse of time. Type II begins to appear after fraction of area of type I becomes maximum. The fraction of area of type II increases with the lapse of time. Fig.6 (c) and (d) show changes in fracture modes of the specimens of 2 1/4Cr–1Mo steel. The changes in the fracture modes are similar to case of 1 1/4Cr–1/2Mo steel. But the time at each type II appears is later then the case of 1 1/4Cr–1/2Mo steel.

Only Type III is observed in the base metal specimens of each steels.

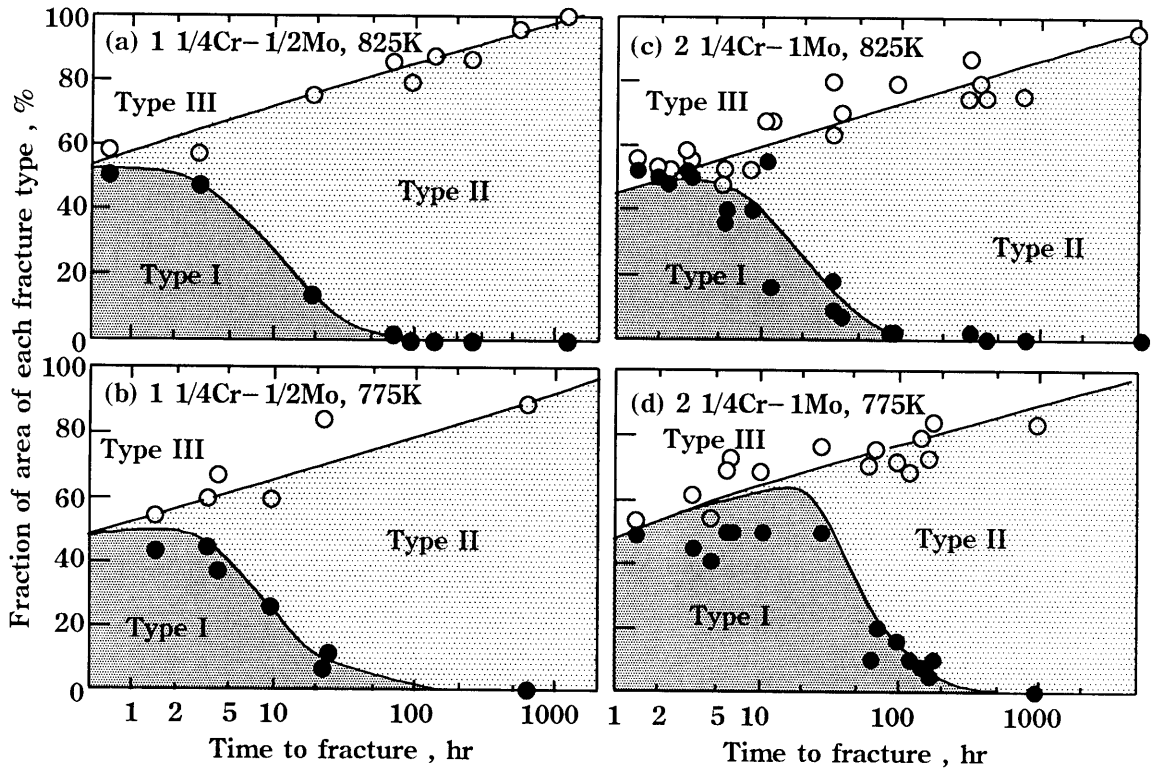

Fig.6 Fraction of areas of fracture types I, II and III; ● fraction of type I, ○ fractions of types I and II.

4. Ductility and fracture mode of SR-treated specimen

4.1 Ductility

Diagrams of stress and the time to fracture of SR-treated specimens of 1 1/4Cr–1/2Mo and 2 1/4Cr–1Mo steels are shown in Fig.7. Results of HAZ specimens are also shown in those figures. In case of 1 1/4Cr–1/2Mo steel (Fig.7(a) and (b)), SR-treated specimen fractured earlier at a given stress than HAZ specimen did in higher stress level. However, it fractured later than HAZ specimen did in low stress level. SR treatment increases time to fracture more remarkably for the test temperature of 775K than for 825K.

In case of 2 1/4Cr–1Mo steel (Fig.7 (c) and (d)), same influence of SR treatment as the case of 1 1/4Cr–1/2Mo steel is observed.

The reduction in area of SR-treated specimen is shown in Fig.8. In case of 1 1/4Cr–1/2Mo steel (Fig.8(a) and (b)), the reduction in area of 200hr-SR is large in all time range. Although the reduction in area of specimens of 2 and 20hr-SR is large in the short time range, it decreases to the value of HAZ specimen when the time to fracture exceeds a certain critical time.

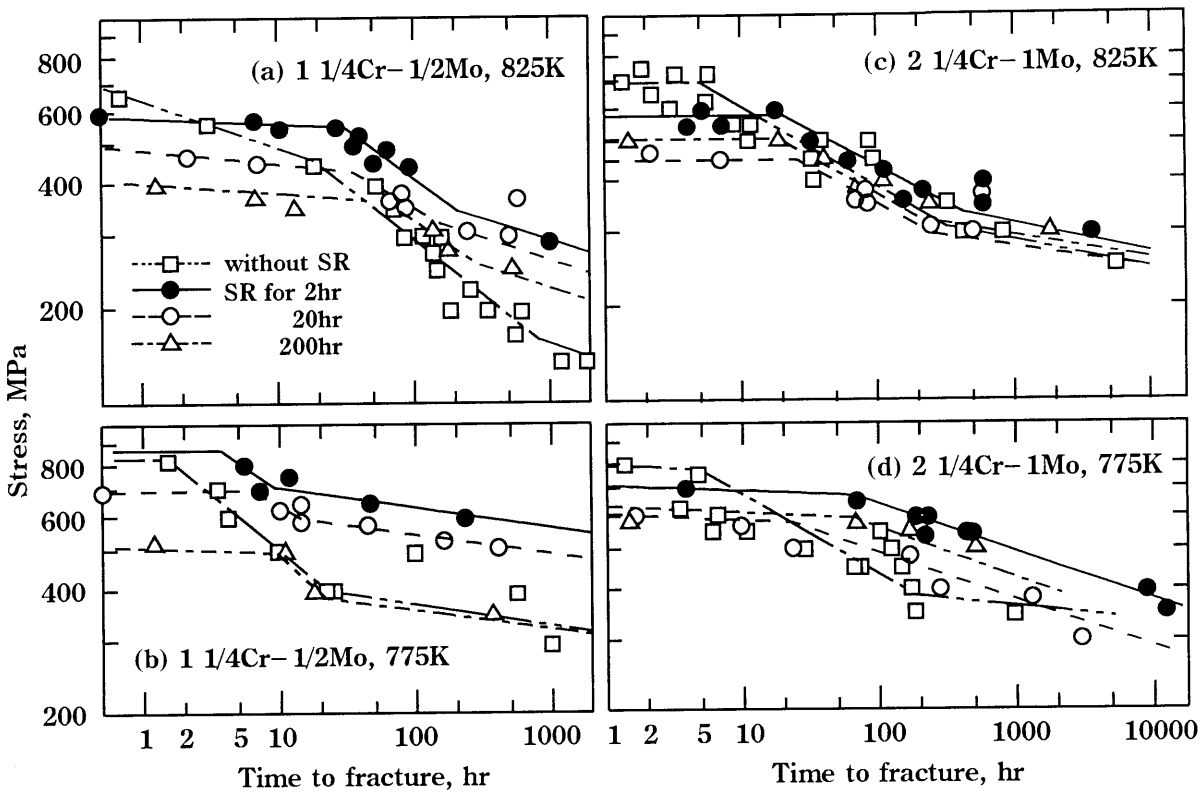

Fig.7 Results of creep-rupture test on SR-treated specimen; 1 1/4Cr-1/2Mo and 2 1/4Cr-1Mo steels.

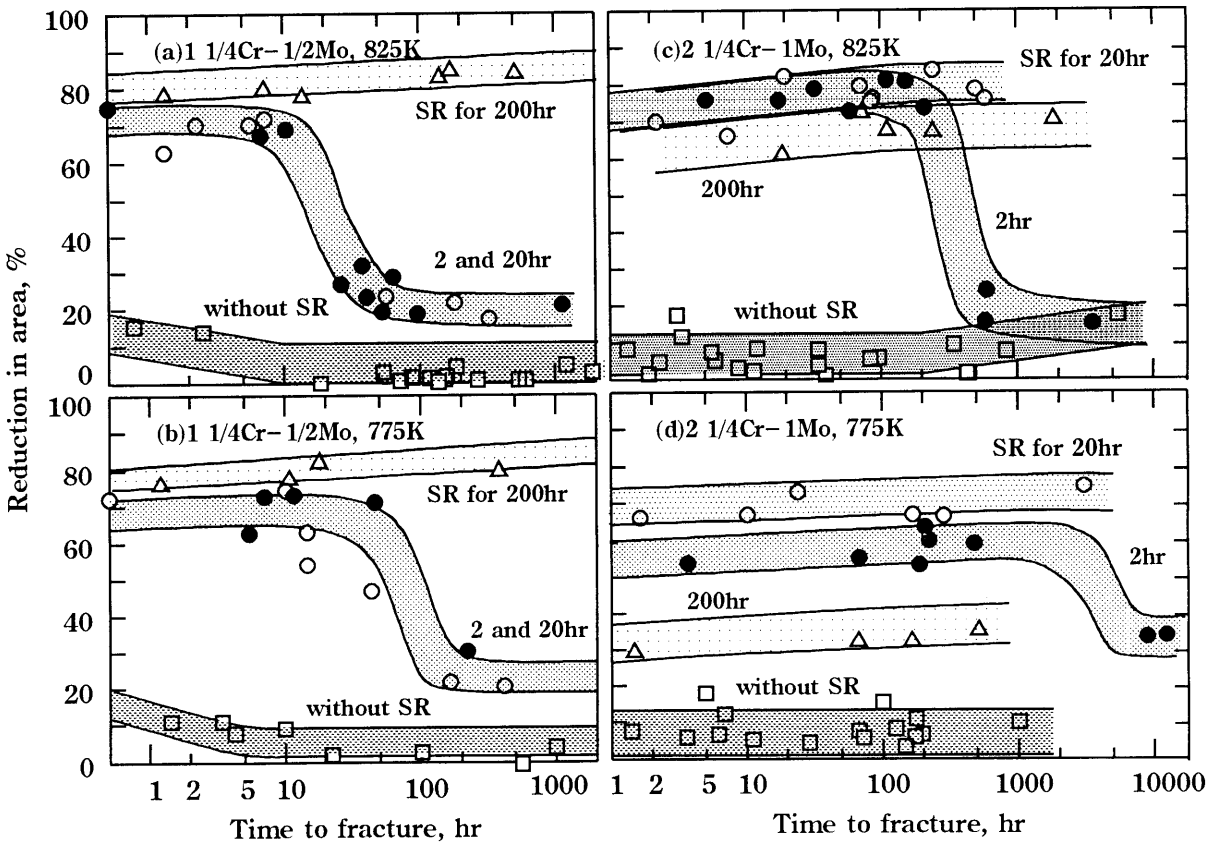

Fig.8 Change in reduction in area with increasing tome to fracture; HAZ and SR-treated specimens; 1 1/4Cr-1/2Mo and 2 1/4Cr-1Mo steel.

In case of 2 1/4Cr–1Mo steel (Fig.8 (c) and (d)), reduction in area is largest for the specimen of 20hr–SR through all time range. For the specimen of 2hr–SR, the reduction in area decreases after certain critical time. for the specimen of 200hr–SR, reduction in area is small even though it does not decrease in the long time range.

Those experimental results inform that the optimum conditions of SR treatment for improving the ductility of HAZ of specimen are 925K for 200hr for 1 1/4Cr–1/2Mo, 975K for 20hr for 2 1/4Cr–1Mo steel.

4.2 Change in fracture mode with the lapse of time

Fracture surfaces of all SR–treated specimens were observed; changes in fracture mode with the lapse of time to fracture at 825K are shown for the specimens of 2 to 200hr–SR as Fig.9. In case of 1 1/4Cr–1/2Mo steel (Fig.9 (a) to (d)), type III alone is observed in short time range. In the specimens of 2 and 20hr–SR type II begins to appear at a critical time. This critical time meets the time at which the reduction in area begins to decrease. In specimen of 200hr–SR, only type III is observed as well in the long time range.

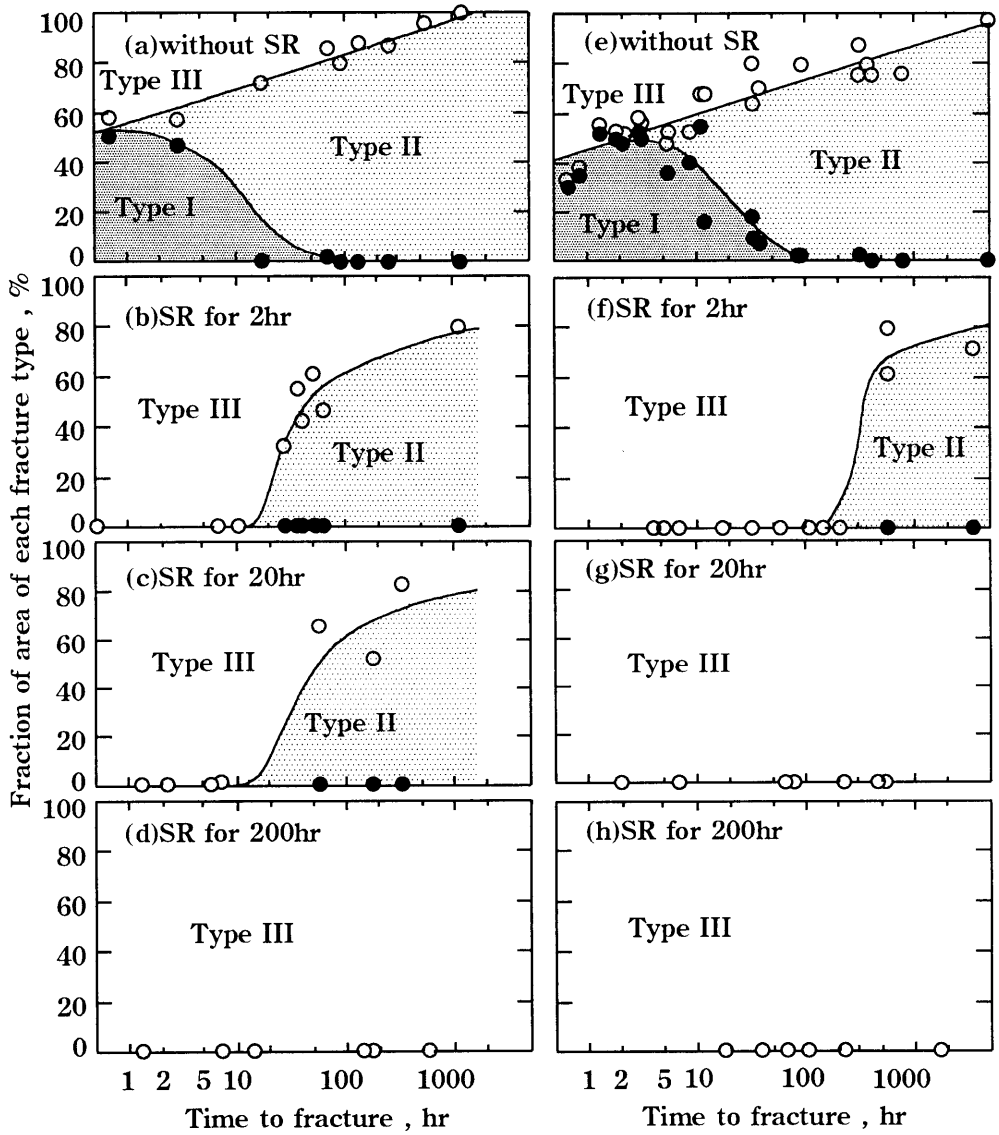

Fig.9 Fraction of areas of types I, II and III; ● fraction of type I, o fractions of type I and II; tested at 825K; (a) to (d): 1 1/4Cr–1/2Mo, (e) to (h): 2 1/4Cr–1Mo steel.

In case of 2 1/4Cr-1Mo steel (Fig.9 (e) to (h)), changes of fracture modes are similar to the case of 1 1/4Cr-1/2Mo steel. In specimen of 2hr-SR, type II appears as well when reduction in area decreases. In specimen of 20 and 200hr-SR, type III alone is observed in all the time range.

Effects of SR treatment on fracture modes are summarized as follows.

(1)Ductile fracture type III alone appears in all the time range in specimen of 20 and 200hr-SR (2 1/4Cr-1Mo steel).

(2)Intergranular fracture type II appears in long time range in specimen of 2 and 20hr-SR, even though type III alone appears in short time range (1 1/4Cr-1/2Mo steel).

(3)The critical time at which type II begins to appear meets well that at which reduction in area decreases abruptly.

(4)Type I disappears by SR treatment.

4.3 Change of hardness

Hardness was measured on HAZ and SR-treated specimens of 2 1/4Cr-1Mo steel. The change of hardness with the lapse of time at 825K is shown in Fig.10. In this figure, the total tempering time which the specimen experienced is taken in abscissa, as the specimen was heated hours before loading. In case of HAZ specimen abnormal increase of hardness is observed in short time range comparing with the normal hardness curve, in which hardness decreases simply with the lapse of tempering time (dotted line [7]). The secondary hardening is induced by precipitation of fine molybdenum carbide, Mo2C replacing pre-existing cementite [8-10].

In case of SR-treated specimens, hardness does not increase in all the time range, except for the earliest one in which hardness increases a little.

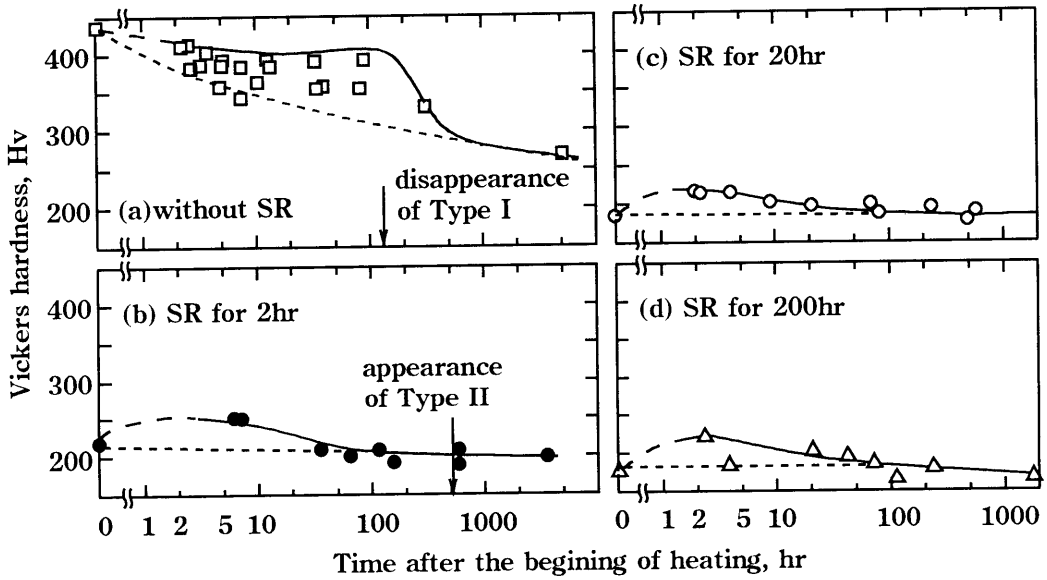

Fig.10 Change in hardness with increasing time to fracture at 825K ; HAZ and SR-treated specimens of 2 1/4Cr-1Mo steel.

5. Consideration for fracture mode

Experimental results informed the following facts.

(1)Intergranular fractures of type I and II arise in HAZ specimen.

(2)Fracture of types I and II disappeared by SR treatment, when the treating time was long enough.

(3)Fracture of type II was revived if the treating time was short. Appearance and disappearance of those fracture types are discussed below from the view point of the relative strengths of ferrite grain and grain boundary.

Fig.11 shows schematically the change of relative strength of ferrite grain and grain boundary with the lapse of time. The strength of ferrite grain is estimated from the change of hardness.

(1)HAZ specimen

Phosphorus is concentrated in grain boundary of prior-austenite by welding (by quenching) and this state is kept in short time range of tempering [11]. This concentration of phosphorus in grain boundary (segregation) reduces the strength of grain boundary much lower than that of ferrite grain (Fig.11(a)). When secondary hardening occurs, the strength of ferrite grain is large enough and typical intergranular fracture, type I appears. When strength of ferrite grain decrease, type II fracture (intergranular fracture accompanied by the deformation of ferrite grains) appears.

(2)Specimen SR-treated for a short time

Phosphorus, which was formerly concentrated in grain boundary by welding, is diffused in some extent from there by SR treatment, and this increases strength of grain boundary much higher than that of ferrite grain (Fig.11(b)). Ductile fracture, type III occurs in ferrite grain in short time

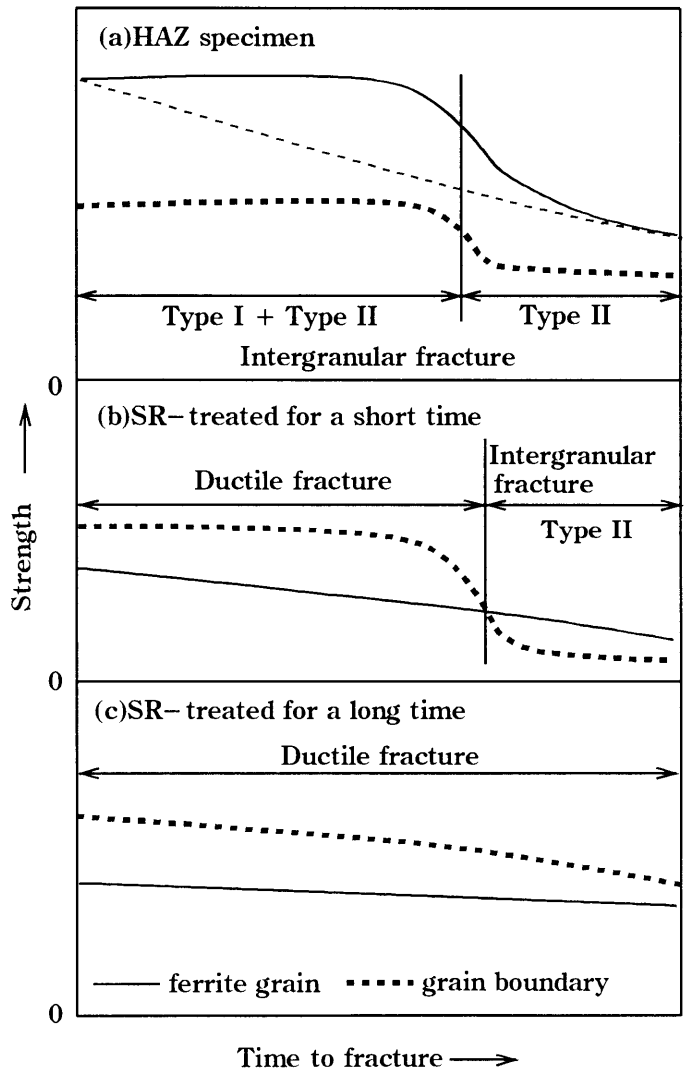

Fig.11 Change in strengthes of grain boundary and ferrite grain with increasing time to fracture (schematic representation).

range. However, phosphorus is concentrated again in grain boundary in the long time range producing the fracture of type II [12].
(3)Specimen SR-treated for a long time
Phosphorus is diffused completely away from grain boundary, and it does not come to there again even though the tempering time is very long in this case. The strength of grain boundary is higher than that of ferrite grain, and hence the fracture occurs in ferrite grain producing type III fracture (Fig.11(c)).

6. Conclusions

Effect of SR treatment on LDCF was investigated by creep-rupture test at 775K and 825K. Experiments were made on synthetic HAZ specimen and specimens SR-treated by several SR conditions. Creep-ductility was discussed in relation to the fracture mode. Results of the experiments are as follows.
(1)LDCF is reproduced by using synthetic HAZ specimen.
(2)Two types of intergranular fractures, type I and II were observed in HAZ specimens.
(3)SR treatment improves ductility.
(4)When the time for SR treatment was long enough, LDCF does not occur in all the time range. But the time was short, LDCF occurs in the long time range producing type II fracture.
(5)Optimum conditions for SR treatment are 925K for 200hr at 1 1/4Cr-1/2Mo and 975K for 20hr at 2 1/4Cr-1Mo steel.

The authors wish to thank Mr. M. Kawakami and Mr. K. Yoshii, the students of Mie University for their cooperations to this research.

References

[1]T.Takamatsu,Y.Otoguro et al.:Effect of metallurgical variables on creep embrittlement of steels, J. Iron and Steel Inst. Japan, 65-7(1979), 851-860 (in Japanese).
[2]T.Takamatsu,Y.Otoguro et al.:The effect of postweld heat treatment on creep embrittlement, J. Iron and Steel Inst. Japan , 67-6(1981), 774-783 (in Japanese).
[3]T.Ishiguro,Y.Murakami et al.:Metallurgical factors affecting the creep ductility of the HAZ of Cr-Mo pressure vessel steels, J. Iron and Steel Inst. Japan, 70-10(1984), 1421-1428 (in Japanese).
[4]Japan Welding Soc.: Yosetsu-Setsugo Binran (Welding Handbook), 1990, p.917 (in Japanese).
[5]K.Tamaki, H.Kawakami, J.Suzuki, N.Akao, Effect of SR treatment on low ductility creep fracture in HAZ of Cr-Mo steel, Document of Int. Inst. Welding, XI-657/96, (1996, Budapest, Hungary).
[6]S.Kinoshita, H.Kaji, M.Katsumata: The relationship between stress-relief embrittlement and temper embrittlement in low alloy steels, Kobe Steel Engineering Reports, Research and Development, 29-4(1979), 67-71 (in Japanese).
[7]E.C.bain: The Alloying Elements in Steel, ASM(1939), 228-231.
[8]K.Tamaki, J.Suzuki et al: Effect of carbides on reheat cracking sensitivity, Trans. Japan Welding Soc., 15-1(1984), 8-16.
[9]K.Tamaki, H.Kawakami, J.Suzuki et al: Temper embrittlement in HAZ of Cr-Mo steels aris-

ing in temperature range of stress relieving, IIW Document IX-1834-96, (1996, Budapest, Hungary).
[10]K.Tamaki, J.Suzuki: Time-Temperature-Hardness Diagram, Res. Rep. Fac. Eng. Mie Univ., Vol.15(1990), 9-22.
[11]K.Tamaki, J.Suzuki, H.Kawakami et al: to be published.
[12]K.Tamaki, H.Kawakami, J.Suzuki: Temper embrittlement in HAZ of Cr-Mo steels, IIW Document IX-1904-98, (1998, Hamburg, Germany).